

# Unsteady natural convection from a horizontal annulus filled with a porous medium

M. Kumari<sup>a,\*</sup>, G. Nath<sup>b</sup>

<sup>a</sup> *Department of Mathematics, Indian Institute of Science, Bangalore 560012, India*

<sup>b</sup> *C/O Dr. S.K. Sinha, KNIT Campus, IV/17, KNIT, Sultanpur 228118, India*

Received 28 April 2006; received in revised form 31 October 2007

Available online 22 April 2008

## Abstract

The unsteady natural convection flow from a horizontal cylindrical annulus filled with a non-Darcy porous medium has been studied. The unsteadiness in the problem arises due to the impulsive change in the wall temperature of the outer cylinder. The Navier–Stokes equations along with the energy equation governing the unsteady natural convection flow have been solved by the finite-volume method. The effect of time variation on the heat transfer is more pronounced only in a small time interval immediately after the start of the impulsive motion and the steady state is reached after certain time. The results show that the annulus completely filled with a porous medium has the best insulating effectiveness. Convection in the horizontal annulus is confined mostly at top and bottom regions. Hence, only these regions should be insulated. In case of annulus partially filled with a porous material, insulating the region near the outer cylinder is more effective than insulating the region near the inner cylinder. The effect of Darcy number on the heat transfer is more pronounced than that of the Grashof number.

© 2008 Elsevier Ltd. All rights reserved.

*Keywords:* Unsteady flow; Natural convection; Horizontal annulus; Porous medium

## 1. Introduction

In recent years, the design of hot-water heating system is based on longitudinal prestressing to limit or prevent longitudinal motion of buried pipe. This eliminates the use of expansion joints or loops. Such a system is known as pipe in pipe system which permits an extension of the allowable temperature range. The system consists of the conveying pipe and the casing pipe which gives the counter force for prestressing. The annulus between the two pipes can be filled completely or partially by an insulating material. The resulting problem can be regarded as a conjugate natural convection problem in a concentric annulus filled with saturated porous medium.

Kuehn and Goldstein [1] have carried out the experimental as well as numerical study of natural convection

from a horizontal cylindrical annuli. Yoo [2] has studied the natural convection flow in a narrow horizontal cylindrical annulus for small Prandtl number. The above problem with porous medium has been studied by several investigators [3–10]. Recently, Aldoss et al. [11] have studied the steady natural convection from a horizontal annulus filled partially or totally with saturated porous medium where the effects of different physical parameters have been examined.

The aim of this study is to consider the unsteady natural convection flow from a horizontal cylindrical annuli filled partially or completely with fluid saturated porous medium. The flow is initially assumed to be steady, but at time  $t^* > 0$  it becomes unsteady due to the sudden change in the wall temperature of the outer cylinder. This causes unsteadiness in the flow field. The Navier–Stokes equations and the energy equation governing the unsteady natural convection flow have been solved by the finite-volume method [12–14]. The steady state results have been

\* Corresponding author. Tel.: +91 80 2293 3214; fax: +91 80 2360 0146.  
E-mail address: [mkumari@math.iisc.ernet.in](mailto:mkumari@math.iisc.ernet.in) (M. Kumari).

## Nomenclature

|                   |  |                      |   |
|-------------------|--|----------------------|---|
| $C$               | dimensionless constant   | $T_i, T_o$           | temperature of the inner and outer cylinders, respectively (K)            |
| $Da$              | Darcy number   | $u^*, v^*$           | velocity components along $r^*$ and $\phi$ directions, respectively (m/s) |
| $F$               | Forchheimer coefficient  | $u, v$               | dimensionless velocity components   |
| $g$               | acceleration due to gravity (m/s <sup>2</sup> )                | <i>Greek symbols</i> |   |
| $Gr$              | Grashof number   | $\alpha$             | thermal diffusivity (m <sup>2</sup> /s)                                   |
| $K$               | thermal conductivity (W/(m K))                                 | $\beta$              | volumetric coefficient of thermal expansion (K <sup>-1</sup> )            |
| $K^*$             | permeability (m <sup>2</sup> )                                 | $\epsilon$           | dimensionless porosity  |
| $Nu$              | Nusselt number   | $\epsilon_1$         | dimensionless constant denoting the change in the wall temperature        |
| $Nu_{cond}$       | Nusselt number for pure conduction state                       | $\theta$             | dimensionless temperature   |
| $\overline{Nu}_i$ | average Nusselt number at the inner cylinder                   | $\mu$                | dynamic viscosity (N s m <sup>-2</sup> )                                  |
| $\overline{Nu}_o$ | average Nusselt number at the outer cylinder                   | $\nu$                | kinematic viscosity (m <sup>2</sup> /s)                                   |
| $\overline{Nu}$   | overall Nusselt number   | $\rho$               | density (kg/m <sup>3</sup> )  |
| $p$               | dimensionless pressure   | $\phi$               | tangential or circumferential direction                                   |
| $p^*$             | pressure (Pa)  | <i>Subscripts</i>    |   |
| $Pr$              | Prandtl number   | f                    | fluid   |
| $r^*$             | radial coordinate (m)  | i                    | inner   |
| $r$               | dimensionless radial distance                                  | inf                  | interface   |
| $r_i^*, r_o^*$    | radii of inner and outer cylinders, respectively (m)           | o                    | outer   |
| $r_i, r_o$        | dimensionless radii of inner and outer cylinders, respectively | p                    | porous medium   |
| $r_{inf}^*$       | interface radius between porous medium and clear fluid (m)     | 1                    | initial condition   |
| $r_{inf}$         | dimensionless interface radius                                 |                      |   |
| $t^*$             | time (s)   |                      |   |
| $t$               | dimensionless time   |                      |   |
| $T$               | temperature (K)  |                      |   |

compared with those of Aldoss et al. [11]. The present results will be useful in the design of heating system, where the wall temperature is subjected to sudden change.

## 2. Analysis

Let us consider an annulus bounded by two horizontal concentric cylinders of radii  $r_i^*$  and  $r_o^*$  (see inset of Fig. 1) which is filled partially or totally with non-Darcy fluid saturated porous medium. Initially ( $t^* = 0$ ), the surface temperatures of the inner and outer cylinders are maintained at  $T_i$  and  $T_o$ , respectively, where  $T_o > T_i$ . This temperature difference gives rise to buoyancy force. At time  $t^* > 0$ , the temperature of the outer cylinder  $T_o$  is suddenly changed which causes unsteadiness in the problem. The fluid is assumed to be incompressible viscous and laminar with constant properties except the density. The thermophysical properties of the fluid and the medium are homogeneous and isotropic. The fluid and solid particles are in local equilibrium which implies equal local temperatures. Inset of Fig. 1 shows the inner layer case where the porous layer is represented by the shaded portion. A cylindrical polar coordinate system ( $r, \phi$ ) is used. Here, we have considered four cases. Case 1: The annulus is filled with a clear fluid, case 2: the annulus is completely filled with a porous med-

ium, case 3: the annulus is partially filled with a porous layer adjacent to the inner cylinder and case 4 which is

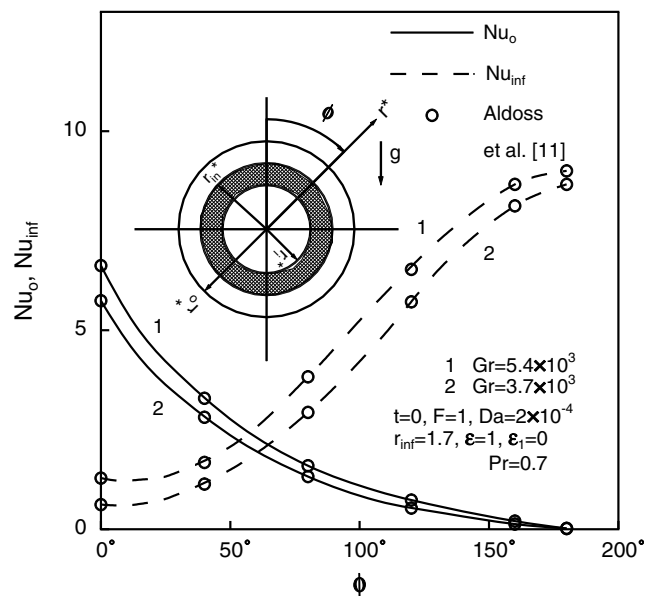


Fig. 1. Comparison of the local Nusselt number at the outer cylinder  $Nu_o$  and at the interface of the porous medium and the clear fluid  $Nu_{inf}$  for the steady flow.

the same as case 3 except that the porous medium is near to the outer cylinder. Under the above assumptions, the Navier–Stokes equations and the energy equation governing the unsteady natural convection flow based on conservation of mass, momentum and energy in dimensionless form are given by [6,8,10,11]

$$\frac{\partial}{\partial r}(ru) + \frac{\partial v}{\partial \phi} = 0, \tag{1}$$

$$\begin{aligned} \epsilon^{-2} \left( \epsilon \frac{\partial u}{\partial t} + u \frac{\partial u}{\partial r} + \frac{v}{r} \frac{\partial u}{\partial \phi} - \frac{v^2}{r} \right) &= Gr\theta \cos \phi - \frac{\partial p}{\partial r} \\ &+ \epsilon^{-1} \left( \frac{\partial^2 u}{\partial r^2} + \frac{1}{r} \frac{\partial u}{\partial r} - \frac{u}{r^2} + \frac{1}{r^2} \frac{\partial^2 u}{\partial \phi^2} - \frac{2}{r^2} \frac{\partial v}{\partial \phi} \right) \\ &- C[Da^{-1} + Da^{-1/2}FQ]u, \end{aligned} \tag{2}$$

$$\begin{aligned} \epsilon^{-2} \left( \epsilon \frac{\partial v}{\partial t} + u \frac{\partial v}{\partial r} + \frac{v}{r} \frac{\partial v}{\partial \phi} + \frac{uv}{r} \right) &= -Gr\theta \sin \phi - \frac{1}{r} \frac{\partial p}{\partial \phi} \\ &+ \epsilon^{-1} \left( \frac{\partial^2 v}{\partial r^2} + \frac{1}{r} \frac{\partial v}{\partial r} - \frac{v}{r^2} + \frac{1}{r^2} \frac{\partial^2 v}{\partial \phi^2} + \frac{2}{r^2} \frac{\partial u}{\partial \phi} \right) \\ &- C[Da^{-1} + FDa^{-1/2}Q]v, \end{aligned} \tag{3}$$

$$\frac{\partial \theta}{\partial t} + u \frac{\partial \theta}{\partial r} + \frac{v}{r} \frac{\partial \theta}{\partial \phi} = Pr^{-1} \left[ \frac{\partial^2 \theta}{\partial r^2} + \frac{1}{r} \frac{\partial \theta}{\partial r} \left( r^{-1} \frac{\partial \theta}{\partial \phi} \right) \right], \tag{4}$$

where

$$\begin{aligned} r &= r^*/R, \quad u = u^*/u_o, \quad v = v^*/u_o, \quad p = p^*/\rho u_o^2, \\ r_{inf} &= r_{inf}^*/R, \theta = (T - T_i)/(T_o - T_i), \quad T_o > T_i, \\ Gr &= g\beta(T_o - T_i)R^3/\nu^2, \quad Da = K^*/R^2, \\ Pr &= \nu/\alpha, \quad t = (\nu/R^2)t^*, \\ R &= r_o^* - r_i^*, \quad Q = (u^2 + v^2)^{1/2}. \end{aligned} \tag{5}$$

The initial conditions (i.e., at time  $t = 0$ ) are given by

$$\begin{aligned} u(r, \phi, 0) &= u_1(r, \phi), \quad v(r, \phi, 0) = v_1(r, \phi), \quad \theta(r, \phi, 0) \\ &= \theta_1(r, \phi), \end{aligned} \tag{6}$$

and the boundary conditions can be expressed as:

$$\begin{aligned} \text{For } t \geq 0, \quad \phi = 0 \quad \text{and} \quad \pi, \quad r_i < r < r_o; \\ \partial u/\partial \phi = \partial v/\partial \phi = \partial \theta/\partial \phi &= 0, \\ \text{for } t \geq 0, \quad r = r_i, \quad 0 < \phi < \pi; \quad u = v = \theta &= 0, \\ \text{for } t \geq 0, \quad r = r_o, \quad 0 < \phi < \pi; \quad u = v = 0, \\ \theta = 1 \text{ for } t = 0, \quad \theta = 1 + \epsilon_1 \text{ for } t > 0, \\ \text{for } t \geq 0, \quad r = r_{inf}, \quad 0 < \phi < \pi; \quad u_f = u_p, \\ v_f = v_p, \quad \theta_f = \theta_p, \\ (\partial v/\partial r)_f &= (\mu_p/\mu_f)(\partial v/\partial r)_p, \\ (\partial \theta/\partial r)_f &= (K_p/K_f)(\partial \theta/\partial r)_p. \end{aligned} \tag{7}$$

The initial conditions ( $u_1(r, \phi)$ ,  $v_1(r, \phi)$  and  $\theta_1(r, \phi)$ ) are given by the steady state equations which are obtained from Eqs. (1)–(4) by putting  $t = \epsilon_1 = \partial u/\partial t = \partial v/\partial t = \partial \theta/\partial t = 0$ .

For applying the above equations in the fluid region,  $\epsilon = 1$  and  $C = 0$  and for the porous region  $C = 1$ . To reduce the complexity of the problem, we have taken the

conductivity and viscosity ratios ( $K_p/K_f$ ,  $\mu_p/\mu_f$ ) to be equal to 1.

The quantities of physical interest are the local and average Nusselt numbers at the inner and outer cylinders as well as the overall Nusselt number which are defined by

$$\begin{aligned} Nu_i &= (r^* \partial T/\partial r^*)_{r^*=r_i^*}/(T_o - T_i) = (r \partial \theta/\partial r)_{r=r_i}, \\ Nu_o &= -(r^* \partial T/\partial r^*)_{r^*=r_o^*}/(T_o - T_i) = -(r \partial \theta/\partial r)_{r=r_o}. \end{aligned} \tag{8a}$$

Now using these equations, the average Nusselt numbers are calculated for each cylinder and they are given by

$$\overline{Nu}_i = \frac{1}{\pi} \int_0^\pi Nu_i d\phi, \quad \overline{Nu}_o = \frac{1}{\pi} \int_0^\pi Nu_o d\phi. \tag{8b}$$

The overall Nusselt number  $\overline{Nu}$  is expressed as

$$\overline{Nu} = (\overline{Nu}_i + \overline{Nu}_o)/2. \tag{8c}$$

The expressions for the local Nusselt numbers at the inner and outer cylinders are essentially same as those of Yoo [2] and Kimura and Pop [6] except that they [2,6] have divided the expressions for the local Nusselt numbers  $Nu_i$  and  $Nu_o$  by  $Nu_{cond}$  ( $= 1/\ln(r_o/r_i)$ ). The local Nusselt numbers  $Nu_i$  and  $Nu_o$  are also same as those of Aldoss et al. [11] except that they have used  $(T_b - T_i)$  in the expressions for  $Nu_i$  and  $Nu_o$  instead of  $(T_o - T_i)$ , where  $T_b$  is the bulk temperature.

### 3. Numerical procedure

Eqs. (1)–(4) under initial and boundary conditions (6) and (7) have been solved by using a finite-volume method. The SIMPLE method of Patanker and Spalding [12] has been used to couple the momentum and continuity equations in a uniform staggered grid. In order to minimize numerical diffusion, the convective terms, in the momentum and energy equations have been discretized using QUICK scheme of Leonard [13] as modified by Hayase et al. [14]. The diffusion terms have been discretized using central difference scheme, whereas a second-order accurate implicit scheme is used for the transient terms. The SIMPLE scheme mentioned above is employed for calculating pressure. Here the under-relaxation factors with values of 0.5, 0.5, 0.7 and 0.35 are used for  $u, v, \theta$  and  $p$ , respectively.

Convergence within each time step is determined through the sum of the absolute relative difference for each dependent variable in the entire flow field

$$\sum_{i,j} \frac{|S_{i,j}^{n+1} - S_{i,j}^n|}{|S_{i,j}^n|} \leq 10^{-5}, \tag{9}$$

where  $S$  represents the dependent variables  $u, v$  and  $\theta$ , the subscripts  $i$  and  $j$  refer to the space coordinates  $(r, \phi)$  and the superscript  $n$  refers to iterative number. Steady state is reached when  $\sum_{i,j} |S_{i,j}^{m+1} - S_{i,j}^m| \leq 10^{-5}$ , where  $m$  refers to the time iteration. Time steps from  $10^{-3}$  to  $10^{-5}$  have been used to insure good accuracy in time. Here  $\Delta r = 0.01$  and  $\Delta \phi = 1^\circ$  are used. A finer grid is used near the walls of the cylinder and at the interface of porous/fluid layer. The

results presented here are independent of grid size at least up to three decimal place.

In order to validate our results, we have compared our steady state results for the local Nusselt numbers at the surface of the outer cylinder ( $Nu_o$ ) and at the interface of the clear fluid and porous medium ( $Nu_{inf}$ ) for  $Gr = 3.7 \times 10^3$  and  $5.4 \times 10^3$ ,  $\epsilon = F = 1$ ,  $Da = 2 \times 10^{-4}$ ,  $r_{inf} = 1.7$ ,  $Pr = 0.7$ . The results are found to be in very good agreement. The comparison is shown in Fig. 1.

#### 4. Results and discussion

Here we have considered the effects of Grashof number  $Gr$ , Darcy number  $Da$  and the interface of the porous medium and clear fluid  $r_{inf}$  on the Nusselt numbers. Also we have taken the porous medium to be polyurethane foam. The Prandtl number for this porous medium saturated with a gas at near standard conditions is 0.5 [5,15]. Hence, we have not shown the effect of the variation of  $Pr$  on the Nusselt number here. However, the Nusselt number increases with  $Pr$ .

The variation of the local Nusselt number at the outer cylinder  $Nu_o$  with time  $t$  ( $0 \leq t \leq 5$ ), when the wall temperature of the outer cylinder is suddenly heated or cooled ( $\epsilon_1 = \pm 0.2$ ), for  $Gr = 3.7 \times 10^3$  and  $5.4 \times 10^3$ ,  $Da = 2 \times 10^{-4}$ ,  $2 \times 10^{-2}$ ,  $\epsilon = 0.9$ ,  $F = 0.55$ ,  $r_{inf} = 1.7$ ,  $\phi = 80^\circ$ ,  $Pr = 0.5$  is shown in Fig. 2. Since significant changes take place in a small time interval ( $0 \leq t \leq 0.5$ ), it is also presented in the inset. When the wall temperature of the outer cylinder is suddenly cooled ( $\epsilon_1 = -0.2$ ), there is a change in the direction of the heat transfer at the surface in a small time interval ( $0 < t < 0.07$ ). However, when

the wall temperature is suddenly increased ( $\epsilon_1 = 0.2$ ), no such phenomenon is observed. The reason for this trend can be explained as follows. At time  $t = 0$ , the temperature of the outer cylinder is higher than that of the fluid near the wall. Hence the heat is transferred from the wall to the fluid (i.e.,  $(\partial\theta/\partial r)_{r=1} < 0$ ). At time  $t > 0$ , the wall is suddenly cooled. Consequently, in a certain small time interval, the temperature of the wall becomes less than that of the fluid near the wall which causes the heat to flow from the fluid to the wall (i.e.,  $(\partial\theta/\partial r)_{r=1} > 0$ ). When the wall is suddenly heated ( $\epsilon_1 = 0.2$ ), no such phenomenon is observed as is evident from the inset of Fig. 2, because the temperature of the wall is always higher than that of the surrounding fluid. The Nusselt number  $Nu_o$  tends to the steady state for  $t > 4$  in a non-monotonic fashion as can be seen from the inset of Fig. 2. Also, the change in the Nusselt number is more pronounced in a small time interval. For a fixed time  $t > 0$ , the Nusselt number  $Nu$  increases with the Grashof number  $Gr$  and the Darcy number  $Da$ . Since the positive buoyancy force ( $Gr > 0$ ) acts like a favourable pressure gradient which accelerated the fluid and reduces both the momentum and thermal boundary layer thickness, the heat transfer is increased. The increase in the Darcy number  $Da$  implies less resistance to the fluid motion which results in thinner boundary layer. Hence the Nusselt number increases with increasing  $Da$ .

Fig. 3 displays the variation of the local Nusselt number at the interface of the porous medium and the clear fluid  $Nu_{inf}$  (case 3) with time  $t$  for  $Gr = 3.7 \times 10^3$  and  $5.4 \times 10^3$ ,  $Da = 2 \times 10^{-4}$  and  $2 \times 10^{-2}$ ,  $F = 0.55$ ,  $r_{inf} = 1.7$ ,  $\epsilon = 0.9$ ,  $\phi = 80^\circ$ ,  $\epsilon_1 = \pm 0.2$ ,  $Pr = 0.5$ . In this case, the change with time is less pronounced as compared to  $Nu_o$ , because the sudden change in the wall temperature

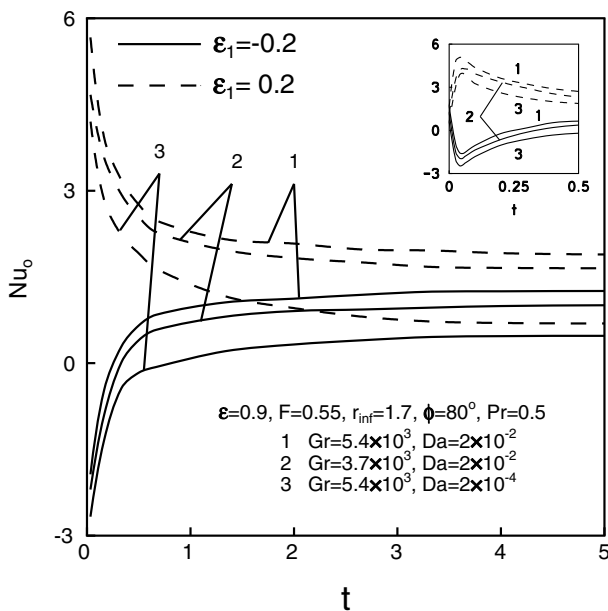


Fig. 2. Variation of the local Nusselt number at the outer cylinder  $Nu_o$  with time  $t$  when the wall temperature of the outer cylinder is suddenly heated or cooled.

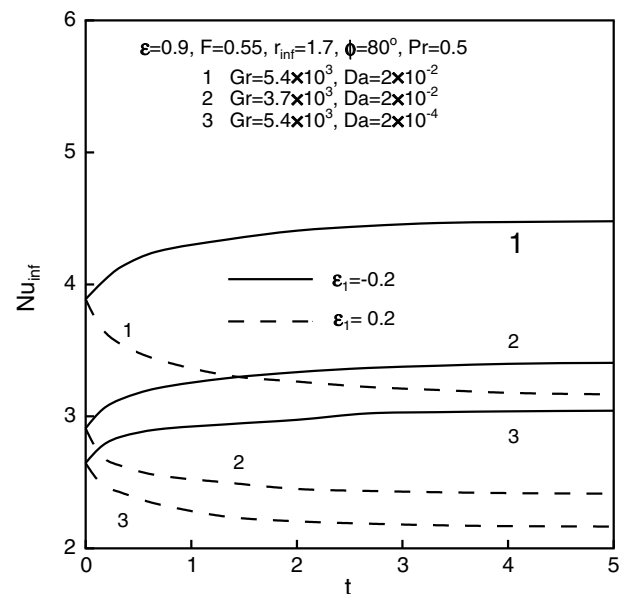


Fig. 3. Variation of the local Nusselt number at the interface of the porous medium and the clear fluid  $Nu_{inf}$  with time  $t$  when the wall of the outer cylinder is suddenly heated or cooled.

of the outer cylinder has an indirect effect on  $Nu_{inf}$ . Further, it increases or decreases with time monotonically. As explained earlier, it increases when the wall is heated, but decreases when the wall is cooled. For a fixed  $\epsilon_1$ ,  $Nu_{inf}$  increases with Grashof and Darcy numbers. The reason for this behaviour has been explained earlier.

Figs. 4 and 5 display the variation of the local Nusselt number at the outer cylinder  $Nu_o$  and at the interface of the porous medium and clear fluid  $Nu_{inf}$  (case 3) with the angular location  $\phi$  ( $\phi = 0$  is the angular position at the top location of the cylinder and  $\phi = 180^\circ$  is the location of the bottom of the cylinder) when  $Gr = 5.4 \times 10^3$ ,  $Da = 2 \times 10^{-2}$ ,  $r_{inf} = 1.3, 1.7$  and  $2.0$ ,  $\epsilon = 0.9$ ,  $F = 0.55$ ,  $t = 4$ ,  $\epsilon_1 = \pm 0.2$ ,  $Pr = 0.5$ . For both wall heating and cooling ( $\epsilon_1 = \pm 0.2$ ),  $Nu_o$  and  $Nu_{inf}$  decrease with increasing radius ratio  $r_{inf}$  ( $r_{inf} = 2$  represents the case of completely filled annulus with porous material (case 2)). This result is important, because it shows that the thicker porous layer has better insulating effect. For a fixed  $r_{inf}$ ,  $Nu_o$  decreases with increasing  $\phi$ , but  $Nu_{inf}$  increases.

Figs. 6 and 7 show the variation of the final steady state ( $t \rightarrow \infty$ ) average Nusselt numbers for both inner and outer cylinders ( $\overline{Nu}_i, \overline{Nu}_o$ ) with the Grashof number  $Gr$  and the Darcy number  $Da$ , respectively, for case 2 (i.e., when the annulus is completely filled with the porous insulating material) when  $\epsilon = 0.9$ ,  $F = 0.55$ ,  $Pr = 0.5$ ,  $t \rightarrow \infty$ ,  $\epsilon = \pm 0.2$ . It is observed that  $\overline{Nu}_i$  and  $\overline{Nu}_o$  in both cases are nearly same which justifies the assumption of the thermal equilibrium of the system i.e., the total heat input rate is the same as the total heat output rate. Similar trend holds good for other cases also, but they are not presented here.

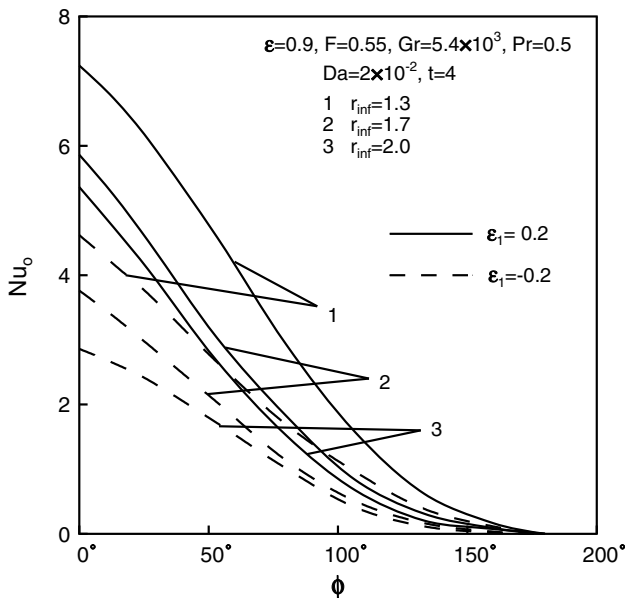


Fig. 4. Variation of the local Nusselt number at the outer cylinder  $Nu_o$  with the angular location  $\phi$  when the wall temperature of the outer cylinder is suddenly heated or cooled.

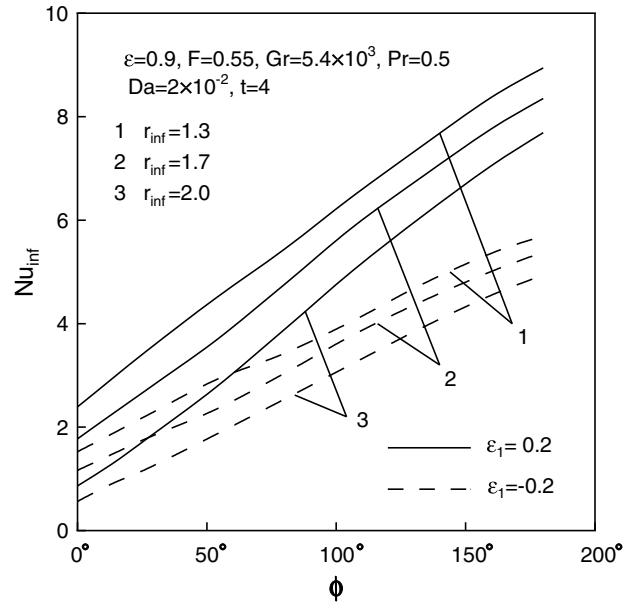


Fig. 5. Variation of the local Nusselt number at the interface of the porous medium and the clear fluid  $Nu_{inf}$  with angular location  $\phi$  when the wall of the outer cylinder is suddenly heated or cooled.

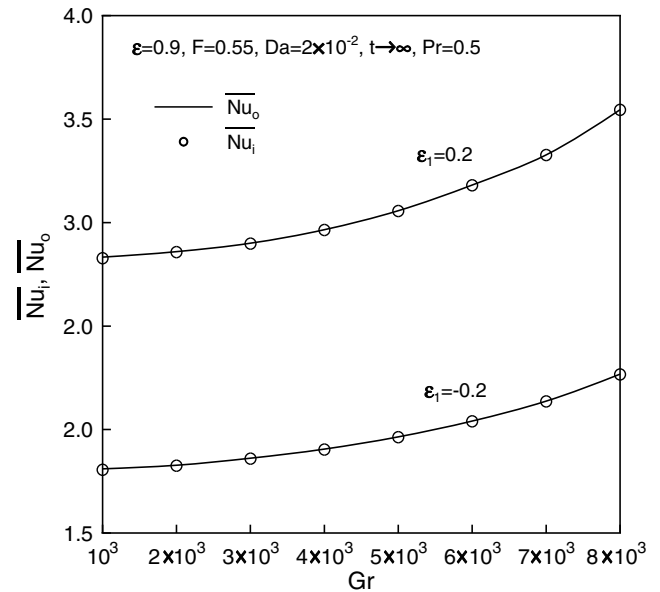


Fig. 6. Variation of the steady state ( $t \rightarrow \infty$ ) average Nusselt numbers at the inner and outer cylinders ( $\overline{Nu}_i, \overline{Nu}_o$ ) with the Grashof number  $Gr$  when the wall of the outer cylinder is suddenly heated or cooled.

Fig. 8 presents the effect of the Grashof number  $Gr$  on the overall Nusselt number  $\overline{Nu}$  for the four cases considered here when  $Da = 2 \times 10^{-2}$ ,  $F = 0.55$ ,  $\epsilon = 0.9$ ,  $t \rightarrow \infty$ ,  $\epsilon_1 = \pm 0.2$ ,  $Pr = 0.5$ . The overall Nusselt number  $\overline{Nu}$  for the case 2 (i.e., when the annulus is completely filled with a porous medium) is less than the other three cases, which indicates that this system is most effective as an insulating system. The next effective insulating system is represented by case 4 where the porous layer is adjacent to the outer cylinder. Case 3 comes next to case 4 and case 1 is the least

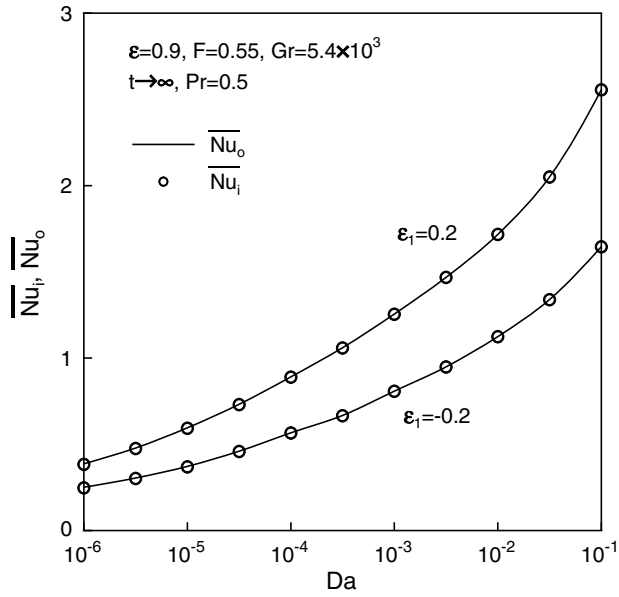


Fig. 7. Variation of the steady state ( $t \rightarrow \infty$ ) average Nusselt numbers at the inner and outer cylinders ( $\overline{Nu}_i, \overline{Nu}_o$ ) with the Darcy number  $Da$  when the wall of the outer cylinder is suddenly heated or cooled.

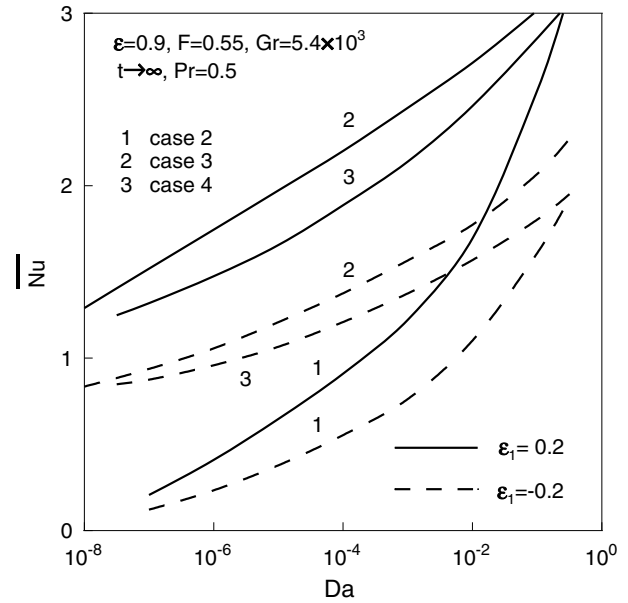


Fig. 9. Variation of the overall Nusselt number  $\overline{Nu}$  with the Darcy number  $Da$  for three cases when the wall of the outer cylinder is suddenly heated or cooled.

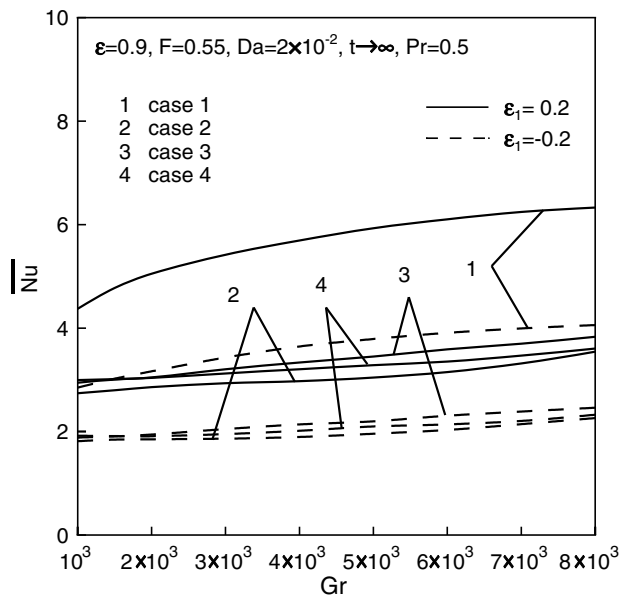


Fig. 8. Variation of the overall Nusselt number  $\overline{Nu}$  with the Grashof number  $Gr$  for four cases when the wall of the outer cylinder is suddenly heated or cooled.

efficient system. The above results hold good for all Grashof numbers  $> 10^3$ . The above behaviour is attributed to the fact that the porous layer suppresses the fluid circulation which leads to reduction in the convective heat transfer. Similar results have been obtained by Aldoss et al. [11] for the steady case.

The effect of the Darcy number  $Da$  on the overall Nusselt number  $\overline{Nu}$  for cases 2, 3, 4 and  $Gr = 5.4 \times 10^3$ ,  $F = 0.55$ ,  $\epsilon = 0.9$ ,  $t \rightarrow \infty$ ,  $\epsilon_1 = \pm 0.2$ ,  $Pr = 0.5$  is shown in Fig. 9. For a fixed  $Da$ ,  $\overline{Nu}$  for case 2 is less than that

of other cases which implies that the annulus completely filled with the porous material is most efficient insulating system and case 4 and case 3 come next in that order. The effect of the Darcy number on  $\overline{Nu}$  is much more pronounced than that of the Grashof number  $Gr$  (see Fig. 8). Also as  $Da$  increases, the difference between the values of the overall Nusselt number  $\overline{Nu}$  for cases 2, 3, and 4 decreases. As  $Da \rightarrow \infty$ , all values should attain the clear fluid limit.

### 5. Conclusions

When the temperature of the outer cylinder is suddenly lowered, there is a change in the direction of the heat transfer in a small time interval immediately after the impulsive reduction of the wall temperature. No such phenomenon is observed when the wall temperature of the outer cylinder is suddenly increased. The final steady state is reached after certain instant of time. The heat transfer is mostly confined at the top and bottom regions of the annulus. Hence, only these regions could be insulated. Annulus completely filled with porous material has the best insulating effect. If the annulus is partly filled with a porous material, then insulating the region near the outer cylinder is more effective than the region near the inner cylinder. The effect of the Darcy number on the average Nusselt Number is more pronounced than that of the Grashof number. The local Nusselt number at the outer cylinder increases with Grashof and Darcy numbers, but it decreases with increasing angular distance ( $\phi$ ). For the steady state case ( $t \rightarrow \infty$ ), the average Nusselt numbers for the inner and outer cylinders are almost same which justifies the assumption of the thermal equilibrium of the system.

## References

- [1] T.H. Kuehn, R.J. Goldstein, An experimental and theoretical study of natural convection in the annulus between horizontal concentric cylinders, *J. Fluid Mech.* 74 (4) (1976) 695–719.
- [2] J.S. Yoo, Natural convection in a narrow horizontal cylindrical annulus:  $Pr \leq 0.3$ , *Int. J. Heat Mass Transfer* 41 (20) (1998) 3055–3073.
- [3] J.P. Caltagirone, Thermoconvective instabilities in a porous medium bounded by two concentric horizontal cylinders, *J. Fluid Mech.* 76 (2) (1976) 337–362.
- [4] P.J. Burns, C.L. Tien, Natural convection in porous media bounded by concentric spheres and horizontal cylinders, *Int. J. Heat Mass Transfer* 22 (6) (1979) 929–939.
- [5] M. Kaviany, Non-Darcian effects on natural convection in porous media confined between horizontal cylinders, *Int. J. Heat Mass Transfer* 29 (10) (1986) 1513–1519.
- [6] S. Kimura, I. Pop, Non-Darcian effects on conjugate natural convection between horizontal concentric cylinders with a porous medium, *Fluid Dyn. Res.* 7 (5–6) (1991) 241–253.
- [7] M.C. Mojtabi, A. Mojtabi, M. Azaiez, G. Labrosse, Numerical and experimental study of multicellular free convection flows in an annular porous layer, *Int. J. Heat Mass Transfer* 34 (12) (1991) 3061–3074.
- [8] J.P.B. Mota, E. Saadjan, Natural convection in a porous, horizontal cylindrical annulus, *J. Heat Transfer* 116 (3) (1994) 621–626.
- [9] W.J. Chang, W.L. Dai, W.L. Chang, The Reynolds number and Prandtl number effects on developing convection of vertical tube partially filled with porous medium, *Int. Commun. Heat Mass Transfer* 23 (4) (1996) 531–542.
- [10] S.C. Halder, Conjugate analysis of heat transfer from a horizontal insulated cylinder, *Int. Commun. Heat Mass Transfer* 30 (1) (2003) 139–147.
- [11] T.K. Aldoss, M. Alkam, M. Shatarah, Natural convection from a horizontal annulus partially filled with porous medium, *Int. Commun. Heat Mass Transfer* 31 (3) (2004) 441–452.
- [12] S.V. Patankar, D.B. Spalding, A calculation procedure for heat, mass and momentum transfer in three-dimensional parabolic flows, *Int. J. Heat Mass Transfer* 15 (10) (1972) 1787–1806.
- [13] B.P. Leonard, A stable and accurate convective modelling procedure on quadratic upstream interpolation, *Comput. Meth. Appl. Mech. Eng.* 19 (1) (1979) 59–98.
- [14] T. Hayase, J.A.C. Humphrey, R. Greif, A consistently formulated QUICK scheme for fast and stable convergence using finite-volume iterative calculation procedure, *J. Comput. Phys.* 98 (1) (1992) 108–118.
- [15] W.M. Kays, M.E. Crawford, *Convective Heat and Mass Transfer*, McGraw-Hill, New York, 1980, pp. 388–391.